Comparative study on the annual performance between loop thermosyphon solar water heating system and conventional solar water heating system

T. Zhang[1,2*], Z.W. Yan[1], L.Y.Wang[1], W.J.Zheng[1], Y.H. Su[2*]

[*1]School of Energy and Mechanical Engineering, Shanghai University of Electric Power, Shanghai City 200090, China

[*2]Department of Architecture and Built Environment, University of Nottingham, Nottingham NG7 2RD, UK

Abstract: Loop thermosyphon (LT) is usually introduced to overcome the freezing and corrosion problems associated with the conventional solar water heating (SWH) system. Compared with the conventional SWH system, the LT-SWH system possesses a lower nighttime heat loss because of the thermal diode property of loop thermpsyphon but bigger daytime heat loss because of the secondary heat exchange. However, the effect of above interaction to the system performance is rarely reported based on long-term running. In this study, based on the typical meteorological year data of Fuzhou city, annual performances of above two systems, including the effective number of supplying days, effective heat gain and nighttime heat loss, are comparatively analyzed under two different operational modes. Variations of above mentioned variables with the increment in the set temperature are discussed. The results indicate that, under the discontinuous heating mode, the effective numbers of supplying days of SWH system and LT-SWH system are 139 and 153, respectively. While the numbers of days are respectively 168 and 173 under the continuous heating mode. The SWH system possesses an expected bigger nighttime heat loss ratio with an average annual value of 15.07% corresponding to 6.15% for the LT-SWH system. Particularly, for the LT-SWH system, the different relative magnitudes of heat loss coefficients functioning at different times leads to a smaller temperature drop at night and also a smaller temperature rise at the subsequent day. It generates an unanticipated results that corresponds to the same month from November to April, the two systems have the approximate effective heat gain. The set temperature significantly influences the relative magnitudes of annual effective number of supplying days and annual effective heat gain, the superiority of LT-SWH system gradually diminishes and even reverses with the increment in the set temperature. The bigger daytime heat loss dominating the dominance is responsible for that transition. Combining with a longer static payback period, it is conditional to substitute the conventional SWH system with the LT-SWH system, especially when the water temperature on demand is high.

Keywords: solar water heating system; loop thermosyphon solar water heating system; typical meteorological year; effective heat gain; nighttime heat loss;

1 Introduction

Renewable energy plays an important role in alleviating the energy crisis. International Energy Agency (IEA) and National Energy Administration of China announced the energy production and consumption of 2018 of China in January 2019. It revealed that renewable energy, especially solar energy and wind power, was becoming competitive with common fossil fuels. China has become the world's biggest source of growth of renewable energy. Among the various utility patterns of solar energy, solar water heating (SWH) systems have been widely used in the fields of building and industrial energy saving (Raisul et al., 2013, Yang et al., 2018, Zhou et al., 2019). It is estimated that a SWH system with 2 m^2 collectors can save ~1500 kWh of electricity per year (Sadhishkumar and Balusamy, 2014).

For a SWH system, there are mainly two heating patterns for the users to acquire hot water on demand. Those are continuous heating mode and auxiliary heating mode. For the former, the users will not consume the water if its temperature on the day does not meet the set value; the mesothermal water will be continually heated the next day or days until its temperature reaches the set value. This mode cannot guarantee the demand of daily hot water and there is considerable nighttime heat loss in the meantime. For the latter, if the water temperature also fails to reach the set value, an auxiliary heater is utilized to guarantee the demand of daily hot water. Ideally, there is no nighttime heat loss under the latter heating pattern; therefore, it possesses the maximum effective heat gain. For convenience, corresponding to the continuous heating mode, the second heating pattern is defined as the discontinuous heating mode in this study.

However, there are corrosion and frost heaving problems accompanied by the conventional SWH system. Furthermore, reverse flow usually occurs in the thermosyphon SWH systems at night (Tang and Yuan, 2014, Morrison,1986, Kok et al., 2015, Rejane et al., 2003, Tang et al., 2010), which leads to a big nighttime heat loss and decreases the effective heat gain (over a 24-h period). Ioannis et al.(2011) experimentally investigated the total nighttime heat loss of three thermosyphon SWH systems. The results indicated that the energy loss at night amounted to an average of 40% of the collected energy in the day. Zhang et al.(2017a) calculated and analyzed the annual performance of an SWH system and found that the average annual heat loss of an conventional SWH system at night accounted for 18% of the collected heat in the day; particularly, the maximum monthly heat loss ratio was bigger than 50%; heat dissipation caused by solar collector accounted for about 87.1% of the total heat dissipation. Tang et al.(2010) respectively established the governing equations for the solar collector, connecting pipes and storage tank to evaluate the nighttime heat loss of a SWH system and found that any effort to increase reverse flow in the system would cause more heat loss to the surrounding from the system, leading to a reduction of the overall thermal efficiency of the system. It is rather apparent that the nighttime heat loss amounts to the largest amount of energy loss of a conventional SWH system under the continuous heating mode.

Loop thermosyphon (LT) is the most appropriate technology to solve the problems associated with a conventional SWH system. Integrating loop thermosyphon with a SWH system, named LT-SWH, can avoid the freezing and corrosion problems by tendentiously filtrating of the refrigerant. And more importantly, thermal diode property of loop thermpsyphon avoids the reverse flow of heat from water tank to solar collector, which is advantageous to reduce the nighttime heat loss. Schematic diagrams of the LT-SWH system and the conventional SWH system can be found in Fig.1. As illustrated in Fig.1, it is effortless to reconstruct a LT-SWH system on the basis of a SWH system by replacing the common water tank with the coil water tank. At the same time, according to the authors' previous work (Zhang et al., 2016), a LT-SWH system can achieve the performance no less than a conventional SWH system. The above advantages suggesting that the LT-SWH system is a promising substitute for domestic hot water supply.

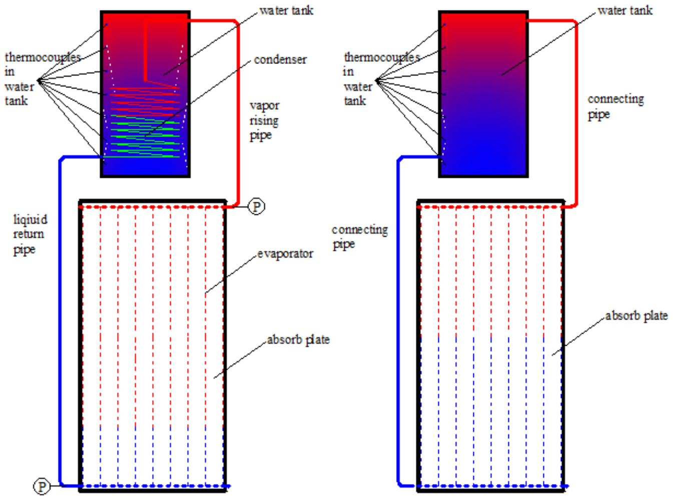

Fig.1 Schematic diagrams of LT-SWH system and conventional SWH system

However, Fig.1 also reveals that the LT-SWH system has a bigger heat loss coefficient in the daytime because of the secondary heat exchange (Zhang et al.,2017b, Nada et al., 2004). And what is more, this disadvantage will be amplified under the continuous heating mode, because the cyclic water temperature under this condition is relatively high. The above shortcomings will further evidently deteriorate the daytime performance of a LT-SWH system.

To the authors' best knowledge, comparisons between the LT-SWH system and the conventional SWH system are mostly under strong solar radiation or short-term operating. The influence of the big heat loss coefficients (at the daytime for the LT-SWH system, while at the nighttime for the SWH system) to the long-term operation is rarely reported. In the present study, based on the typical meteorological year data of Fuzhou city, annual performances of that two systems under the continuous heating mode and the discontinuous heating mode are comparatively studied. Variations in effective number of supplying days, effective heat gain and nighttime heat loss are displayed and discussed in detail. Influences of the set temperature to the relative magnitude of these three variables are also presented.

2 Mathematical model

2.1 Evaluation of daytime performance

The daytime photothermal efficiency of a solar thermosyphon system, η_t, can be calculated as followed (Huang and Du, 1991):

$$\eta_t = \alpha - U \frac{T_i - \overline{T_a}}{H_T} \tag{1}$$

where $\overline{T_a}$ is the daily average ambient temperature, °C; H_T is the daily cumulative solar radiation on the collector surface, MJ/m^2; T_i is the initial water temperature, °C; α is the typical photothermal efficiency when the initial water temperature equals the daily average ambient temperature; U is the daytime heat loss coefficient. The values of α and U can be obtained by linear fitting based on the experimental data. The obtained regression equation can be used to estimate the photothermal efficiency of the system under different climatic conditions.

Normally, the solar collector is installed with inclination. However, the solar radiation contained in the weather data of typical meteorological year refers to that projecting on the horizontal plane. Therefore, solar radiation on the inclined surface, H_T, has to be calculated on the basis of the data on the horizontal surface, which can be expressed as (Qiu et al., 2001):

$$H_T = R_b(H_c - H_{cd}) + H_{cd}\frac{1+\cos\beta}{2} + H_c\rho\frac{1+\cos\beta}{2} \tag{2}$$

$$R_b = \frac{\frac{\pi}{180}\omega_s^{'}\sin(\varphi-\beta)\sin\delta + \cos(\varphi-\beta)\cos\delta\sin\omega_s^{'}}{\frac{\pi}{180}\omega_s\sin\varphi\sin\delta + \cos\varphi\cos\delta\sin\omega_s} \tag{3}$$

$$\omega_s^{'} = \min[\cos^{-1}(-\tan\varphi\tan\delta), \frac{\pi}{2}] \tag{4}$$

$$\omega_s = \cos^{-1}(-\tan\varphi\tan\delta) \tag{5}$$

$$\delta = 23.45\sin\frac{360(284+n)}{365} \tag{6}$$

where H_c is the solar radiation on the horizontal plane, W/m^2; H_{cd} is the scattering radiation on the horizontal plane, W/m^2; ρ is the reflectivity of ground, normally the value is 0.2; R_b is the ratio of direct radiation that respectively projected on the inclined surface and the horizontal plane; φ is the geographical latitude; β is the inclination angle of solar collector; δ is the solar declination angle; ω_s is the hour angle of sunrise and sunset on the horizontal plane; $\omega_s^{'}$ is hour angle of sunrise and sunset on the inclined plane; n is the serial number in the year.

To make sense of the results, the SWH system and the LT-SWH system with approximate typical photothermal efficiencies are invited for comparison. Their performances can refer to He et al. (2011) and Zhang et al. (2016), which are:

$$\text{SWH system} \qquad \eta_{t,SWH} = 0.547 - 0.052\frac{T_i - \overline{T_a}}{H_T} \tag{7}$$

$$\text{LT-SWH system} \qquad \eta_{t,LT-SWH} = 0.550 - 0.140\frac{T_i - \overline{T_a}}{H_T} \tag{8}$$

From Eqs. (7-8), one can reconfirm that the LT-SWH system has a bigger heat loss coefficient because of the secondary heat exchange.

2.2 Evaluation of nighttime heat loss

Under the continuous heating mode, the final water temperature at the end of the day fails to reach the set value with a high-probability if the solar radiation is weak or the initial water temperature is low. Nighttime heat loss should be therefore taken into account to calculate the initial water temperature of the next day. However, to the authors' best knowledge, although there were several experiments involve the influence of the reverse flow to the solar thermosyphon system, none of semi-empirical correlations for the nighttime heat loss were proposed.

Tang et al. (2010) acquired the key coefficients for the governing equations from their experiments. However, their methods cannot directly shift to the present study. Instead, nighttime heat loss coefficients are calculated based on published semi-empirical correlations in this study.

For the solar collector at overcast nights, the heat loss by thermal radiation from the collector surface to the sky dome is negligible, and heat loss (unit time) from collector to the enviroment can be expressed by (Tang et al., 2010):

$$mC_p\Delta T = A_c U_l\left(T_p - T_a\right) \tag{9}$$

where m is the mass of water inside the collector, kg; A_c is the area of solar collector, m^2; U_l is the heat loss coefficient of solar collector, W/(m^2•K); T_p is the average temperature of the absorbing plate, ℃;

For the solar collector, the heat loss is mainly through top, back and edge of it. The heat loss coefficient of the top can be calculated as follows (Klein, 1975):

$$U_t = \left\{\frac{N}{\frac{c}{T_p}\left[\frac{T_p-\overline{T_a}}{N+f}\right]^e} + \frac{1}{h_w}\right\}^{-1} + \frac{\sigma(T_p+\overline{T_a})(T_p^2+\overline{T_a^2})}{(\varepsilon_p+0.00591Nh_w)^{-1}+\frac{2N+f-1+0.133\varepsilon_p}{\varepsilon_c}-N} \tag{10}$$

$$f = (1+0.0892h_w - 0.1166h_w\varepsilon_p)(1+0.07866N) \tag{11}$$

$$c = 520(1-0.000051\beta^2) \tag{12}$$

$$e = 0.43(1-100/T_p) \tag{13}$$

$$h_w = 5.7+3.8V \tag{14}$$

where N is the number of the glass cover, and usually N=1; ε_p is the emissivity of the absorbing plate, -; ε_c is the emissivity of the glass cover, -; V is the wind speed, m/s; σ is the Boltzmann constant. The value of T_p is assumed as the average water temperature at the beginning and at the end of the tank during the corresponding time.

While the heat loss coefficient of the back of the solar collector consists of the heat conduction resistance of the insulation material and the convective heat resistance between the solar collector and the environment (Zhang, 2004):

$$U_b = \frac{1}{h_w + L_b / \lambda_b} \tag{15}$$

where L_b is the thickness of the thermal insulation layer, m; λ_b is the thermal conductivity of the insulation layer, W/(m·K).

The heat loss coefficient of the edge of the solar collector can be approximately estimated by:

$$U_e = \left(\frac{\lambda_e}{L_e}\right)\left(\frac{A_e}{A_c}\right) \tag{16}$$

where A_e is the total area of the edge of the solar collector, m^2. Usually, insulation materials filled within the edge and the back of the solar collector are the same. The physical parameters in Eq.(15) and Eq.(16) are therefore same too.

The total heat loss coefficient of solar collector is therefore as:

$$U_l = U_t + U_b + U_e \tag{17}$$

However, at clear nights, the situation is different, part of thermal radiation emitted from the absorber will directly pass through the glass cover and dissipate into the sky dome due to the fact that the glass cover used in collectors is not perfectly opaque for the long-wave thermal radiation (Cook, 1985). Therefore, the heat loss of solar collector in this case can be expressed by:

$$mC_p\Delta T \approx A_c U_l \left(T_p - T_a\right) + A_c \tau \left[\varepsilon_p \sigma \left(T_p + 273.15\right)^4 f_{abs-sky} - Q_{sky}\right] \tag{18}$$

$$f_{abs-sky} = 0.5\left(1 + \cos\beta\right) \tag{19}$$

where τ is transmittance of glass cover, -; T_a is real-time ambient temperature, ℃; Q_{sky} is the thermal radiation projects on the collector surface from the sky dome, J/m^2. The premise of calculating Q_{sky} needs to measure the incident thermal radiation from the sky dome at night. However, there is also no relevant data of long-wave radiation. Instead, the Q_{sky} is therefore calculated as following (Duffie and Beckman, 2006):

$$Q_{sky} = \sigma T_{sky}^4 \tag{19}$$

$$T_{sky} = 0.0552 T_a^{1.5} \tag{20}$$

For the connecting pipes, only the heat conduction resistance of the insulation material and the convective heat resistance between the pipes and environment are considered, that is:

$$U_p = \frac{1}{h_w + \frac{\ln D_o / D_i}{2\pi\lambda_p}} \tag{21}$$

For the water tank, Fan and Furbo(2012a) experimentally studied the temperature-dependent heat loss coefficients for different parts of the water tank. The total heat loss coefficient is expressed as:

$$U_w = 2.4 + 0.00198\Delta T \tag{22}$$

The water tank should be recharged in the next morning if the hot water was used up at night. However, the temperature data of municipal water is not including in the data of a typical meteorological year. Alternatively, the water temperature of the local river is employed. Li et al. (2006) established a correlation to estimate the water temperature of the river in China by using the meteorological factors. The influences of ambient temperature, humidity and wind speed were comprehensively taken into account in the semi-empirical correlation, which can be expressed as:

$$T_i = 4.717e^{0.041T_a}\left(\frac{(1+r^2)^{0.781}}{(1+0.325V^2)^{0.0325}}\right) \tag{23}$$

where r is relative humidity of ambient air, -.

3 Settings of simulation and validation of nighttime heat loss

3.1 Simulation settings

Volume of water tank and the area of solar collector are set same to references (Zhang et al., 2016, Fan and Furbo, 2012a), that are 150 L and 2 m^2. According to Chinese standard, it is exactly applicable to a typical Chinese family of three or four people (Wang and Wang, 2008). The minimum water temperature on demand is set at 48 ℃ (GB/T, 19141-2003). When calculating the nighttime heat loss, values of the parameters of the SWH system and LT-SWH system are shown in table 1. The inclination angle of the solar collector is set at 40°, which is equal to the LT-SWH collector in Zhang et al. (2016) and a little bigger than that of the SWH collector in He et al. (2011).

When calculating the annual performances of SWH system and LT-SWH system, the following assumptions are made:

1) The hot water will be used at night only when the temperature is higher than the set value

and will be used up that night. In addition, the hot water is used up within a short time, the heat loss during this time is therefore negligible.

2) Water is recharged and nighttime temperature drop is stopped both at the sunrise time of the next day. That is when solar radiation is bigger than zero. Besides, the charging time is ignored.

3) Eqs.(7-8) predict the photothermal performances of the whole daytime; thus, only the final water temperature can be predicted. Under the circumstances, the final water temperature can be higher than the set value and the effective heat gain is also calculated based on the actual final temperature, not the set value.

4) The nighttime temperature drop is limited. The water temperature cannot be lower than the ambient temperature and cannot be below 0 ℃ at the same time.

Table 1. Parameter values of the SWH system and the LT-SWH system

System	ε_p	ε_c	L_b (m)	λ_b W/(m·K)	D_o mm	D_i mm
SWH	0.05	0.82	0.05	0.04	40	20
LT-SWH	0.05	0.82	0.05	0.04	40	20

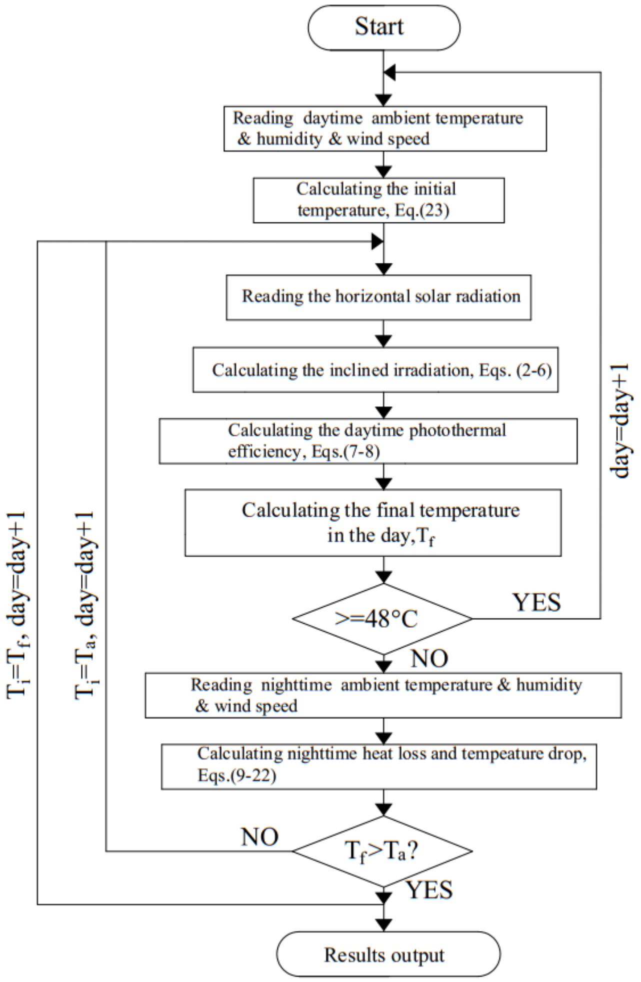

Fig.2. Flow chart of calculation of the annual system performance

A C++ program is developed to precalculate the average daytime ambient temperature, to read the meteorological data, to calculate the photothermal performance of daytime and heat loss of nighttime. The flow chart of the annual performance under the continuous heating mode is displayed in Fig.2. Because the flow chart of the discontinuous heating mode is relatively simple, it is not listed here.

3.2 Validation of nighttime heat loss

As mentioned before, Eqs. (7-8) were fitted based on the actual outdoor tests. Therefore, only the nighttime heat loss performances of the two systems need to be validated. For the LT-SWH system, the data were obtained from authors' previous experiments and the experimental setup can be found in Zhang et al. (2016) in detail. For the SWH system, the nighttime data are provided by Yang Zhang (He et al., 2011). Meanwhile, variables initialized in simulation are all corresponding to their experimental setup. The results are presented in Fig.3 in detail.

From Fig.3, one can see that the simulation results of nighttime temperature performance both agree well with the experimental data, the mean deviations of the two systems are both less than 1.5%. Meanwhile, from the illustration in the bottom left corner, one can obviously observe the ups and downs in water temperature to a small extent, which indicates that reverse flow occurs in the water tank. However, the forming mechanisms are different. For the LT-SWH system, it is mainly determined by the internal flow within the water tank (Fan and Furbo, 2012a, Fan and Furbo, 2012b). While for the SWH system, the effect of relative height between the water tank and the collector (Morrison, 1986), as well as the heat loss through connecting pipes (Vaxman and Sokolov, 1986), should be additionally considered.

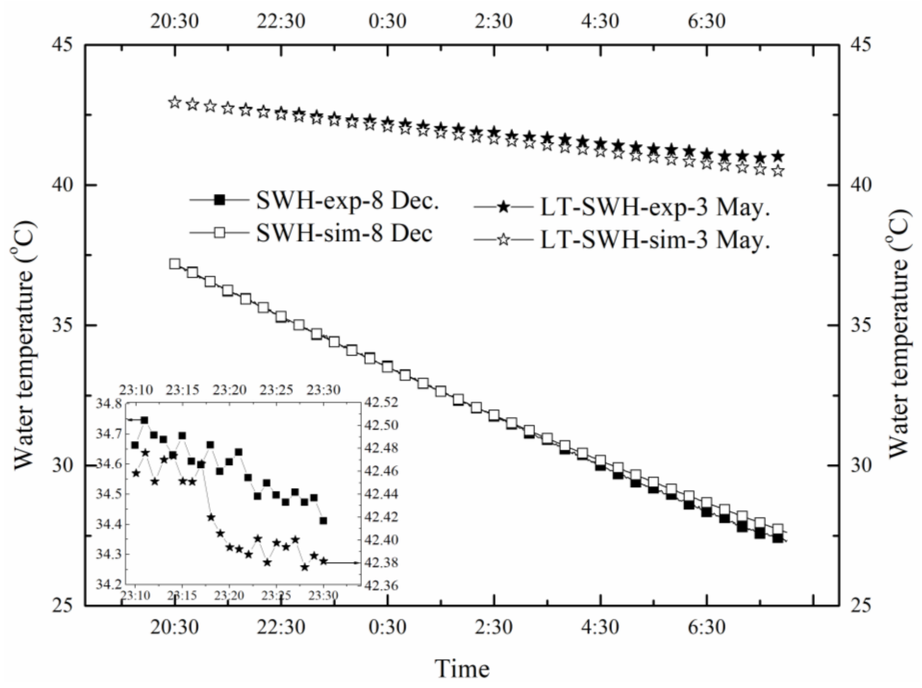

Fig.3. Validation of the nighttime heat losses of SWH system and LT-SWH system

4 Result and discussion

Fuzhou city (26.08ºN,119.30ºE), which is the provincial capital of Fujian province in China, belongs to the subtropical zone enjoying a humid monsoon climate. Fig.4 illustrates the average monthly direct radiation ratio, the monthly average ambient temperature in Fuzhou city, as well as the monthly cumulative solar radiation projecting on the horizontal plane and the inclined plane. One can note that the monthly average R_b displays a trend of decreases first and then increases with month; the value ranges between 0.85-1.85 and the maximum and minimum values corresponding to December and June, respectively. It is because the value of R_b is determined by the solar declination angle δ, the hour angle of sunrise and sunset respectively on the inclined plane ω'_s and on the horizontal plane ω_s. However, the values of ω'_s and ω_s vary with the solar declination angle δ and the geographical latitude ϕ. When $0° < \delta < 23°24'$, ω'_s equals to $\pi/2$, while ω_s increases with the increasing of δ; thus, during the spring equinox to the summer solstice, R_b gradually decreases with increasing the δ. When $-23°24' < \delta < 0°$, ω'_s equals to ω_s, and ω'_s decreases with the increasing of δ; Therefore, during the autumnal equinox to the winter solstice, R_b gradually increases with decreasing the δ. While during the winter solstice to the spring equinox, R_b gradually decreases with increasing the δ.

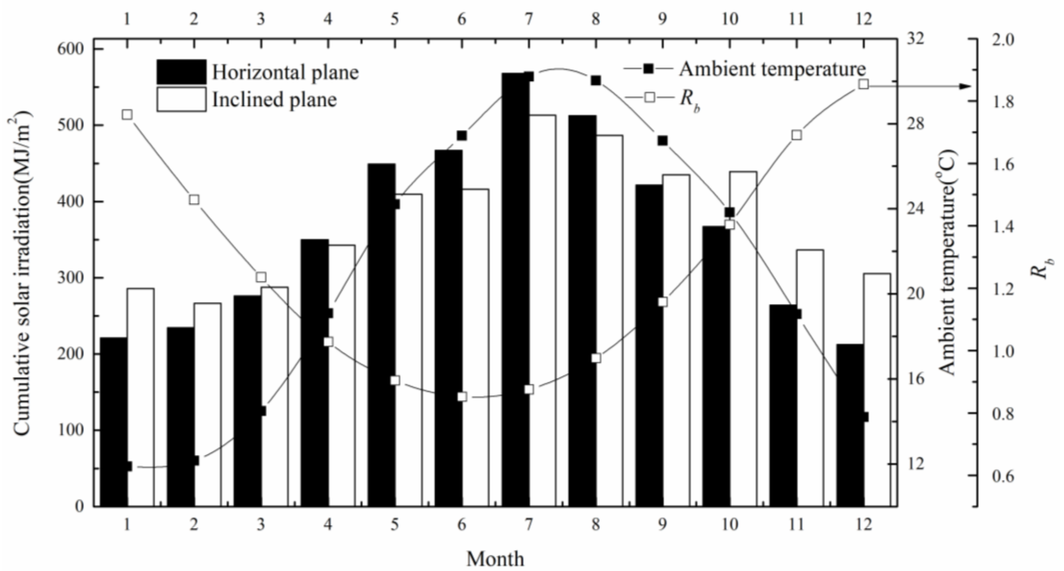

Fig.4. Variations in monthly average ambient temperature, R_b, monthly cumulative solar radiation

The average monthly ambient temperature, which displays an overall trend of increases first and then decreases, ranges between 11.9 °C and 30.2 °C; the minimum and maximum values are corresponding to January and July, respectively.

For solar radiation projecting on the inclined surface, it can be seen from Eq. (2) that, when the collector inclination angle β is constant, it is linearly dependent on the direct radiation ratio, R_b. Therefore, its magnitude is directly influenced by R_b. During May to August, R_b is less than 1, the cumulative solar radiation on the inclined plane is, therefore, lower than that of on the horizontal plane; while the other months are on the contrary. By calculation, the monthly cumulative solar radiation on the inclined surface ranges between 266.6 MJ/m^2 and 513.4 MJ/m^2; the maximum and minimum values are respectively corresponding to July and February. Yearly cumulative solar radiation on the inclined plane is 4524.6 MJ/m^2, which is slightly larger than that on the horizontal plane corresponding to 4343.4MJ/m^2.

4.1 Comparison of the effective number of supplying days and effective heat gain

When only solar energy is used, the monthly effective number of supplying days of the SWH system and the LT-SWH system, under different heating modes, are presented in Fig.5. The effective supplying day is defined as the day on which the water temperature is higher than the set value.

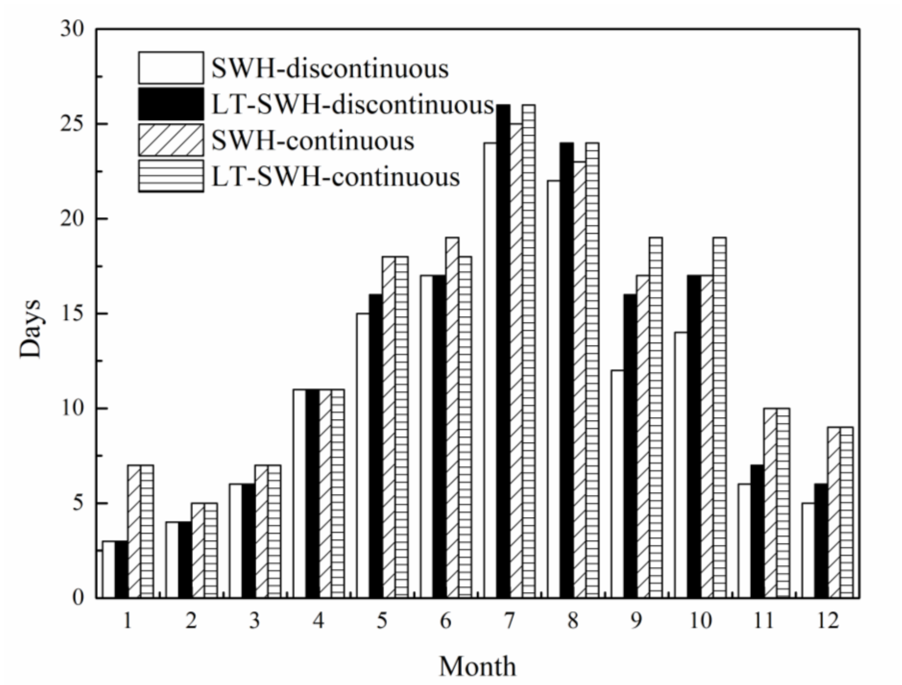

Fig.5. Comparison of the monthly effective numbers of supplying days under different heating modes

Fig.5 indicates that except June under the continuous heating mode, the effective number of supplying days of LT-SWH system is always no less than that of the SWH system corresponding to the same month. The comparatively higher photothermal efficiency of the LT-SWH system is responsible for that. Meanwhile, for the same system, the effective number of supplying days of the discontinuous heating mode is always less than the continuous heating mode. It is understandable that the accumulation of heat, under the continuous heating mode, increases the effective number of supplying days and this effect is more obvious in the months with low ambient temperature or weak solar radiation.

Furthermore, it can be seen from Fig.5 that the maximum values of the effective number of supplying days are all taken in July, regardless of the systems and the heating modes. However, the minimum values are taken in different months, which is in January under the discontinuous heating mode and in February under the continuous heating mode. It has been calculated that, under the discontinuous and continuous heating modes, the annual effective numbers of supplying days for the SWH system are 139 and 168, respectively; while for the LT-SWH system, they are 153 and 173, respectively.

It is also understandable that due to the high initial water temperature and strong solar radiation in summer, the effective numbers of supplying days corresponding to the same month but different heating modes are approximate.

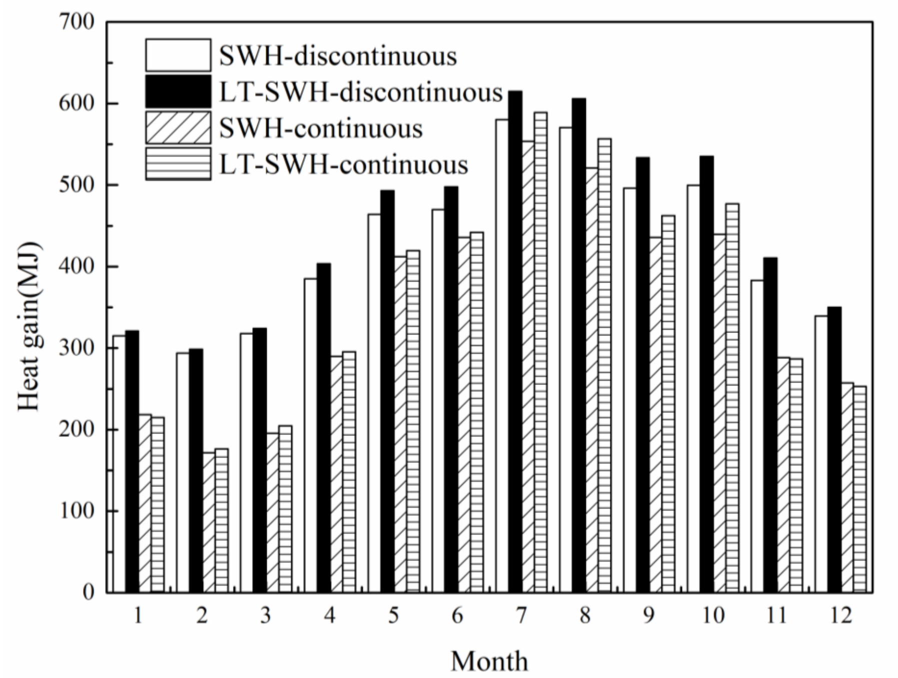

Fig.6. Comparison of the monthly effective heat gains under different heating modes

Under different heating modes, the effective heat gains are illustrated in Fig.6 in detail. It shows that firstly, corresponding to the same month, the effective heat gain takes a bigger value under the discontinuous heating mode, which is different from the trend of the effective number of supplying days. It is mainly because, according to the assumption, there is no nighttime heat loss under this condition. Secondly, the maximum and minimum heat gains take in July and February, respectively.

Thirdly, Fig.6 shows that under the discontinuous heating mode, the effective heat gain of the SWH system is always smaller than that of the LT-SWH system corresponding to the same month. It is also because, under this circumstance, the daytime photothermal efficiency of LT-SWH system is bigger.

However, under the continuous heating mode, one can note that from November to April, the effective heat gain of the SWH system is approximate to that of the LT-SWH system corresponding to the same month; meanwhile, the relative magnitudes are tangled. Nevertheless, under the other months, the relative magnitudes of the effective heat gain between the SWH system and the LT-SWH system share the similar trend with the discontinuous heating mode. Following, the reasons for the unforeseeing will be analyzed in detail by the performs of water temperature and nighttime heat loss.

4.2 Comparison of the nighttime heat loss

As mentioned before, heat loss at night leads to a lower effective heat gain under the continuous heating mode. The specific values of the monthly cumulative heat loss under different heating modes, as well as the average monthly temperature drops at night, are displayed in Fig.7 in detail.

Fig.7 clearly shows that firstly, the nighttime heat loss and temperature drop of the SWH system are obviously bigger than that of the LT-SWH system corresponding to the same month. The maximum values are both taken in February with the value of 93.4 MJ and 39.7 MJ, respectively; while the minimum values are both taken in July with the value of 17.1 MJ and 5.6 MJ, respectively. Secondly, both of the two systems have a bigger cumulative heat loss from November to April. It is because, combining with Fig.5, the effective numbers of supplying days during these months are limited due to the comparatively weak solar radiation and low ambient temperature; in addition, the comparatively low nighttime ambient temperature leads to a bigger heat loss coefficient and further leads to a bigger nighttime cumulative heat loss. However, from May to October, especially in July and August, because of the strong solar radiation and high initial water temperature, water temperature at the end of the day reaches the set value on most of the days, which decisively reduces the nighttime heat loss; besides, the high ambient temperature at night also plays a role in reducing the nighttime heat loss.

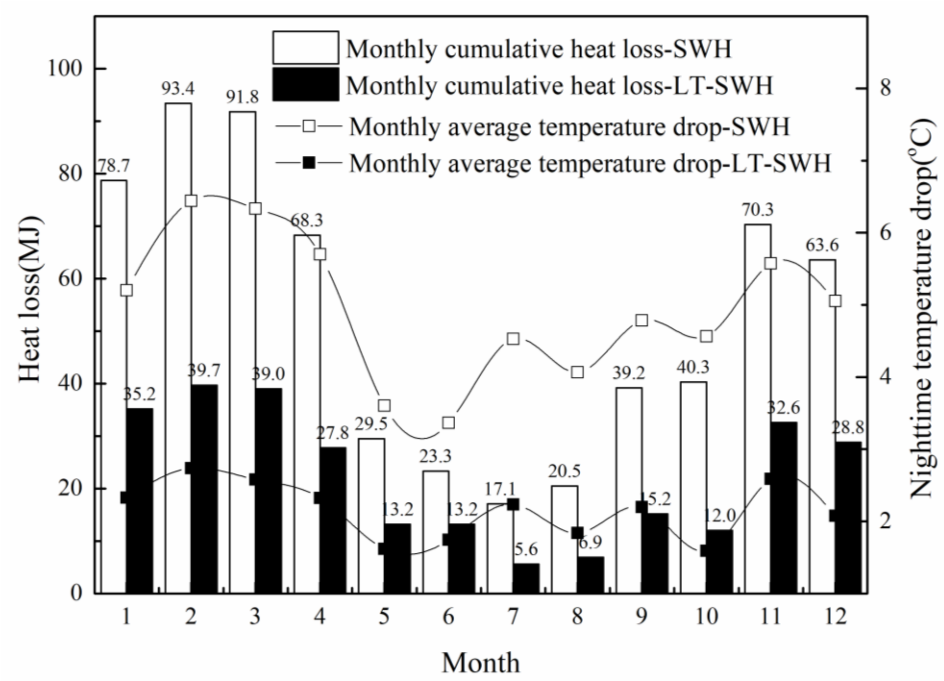

Fig.7. Comparison of monthly cumulative heat loss and monthly average temperature drop

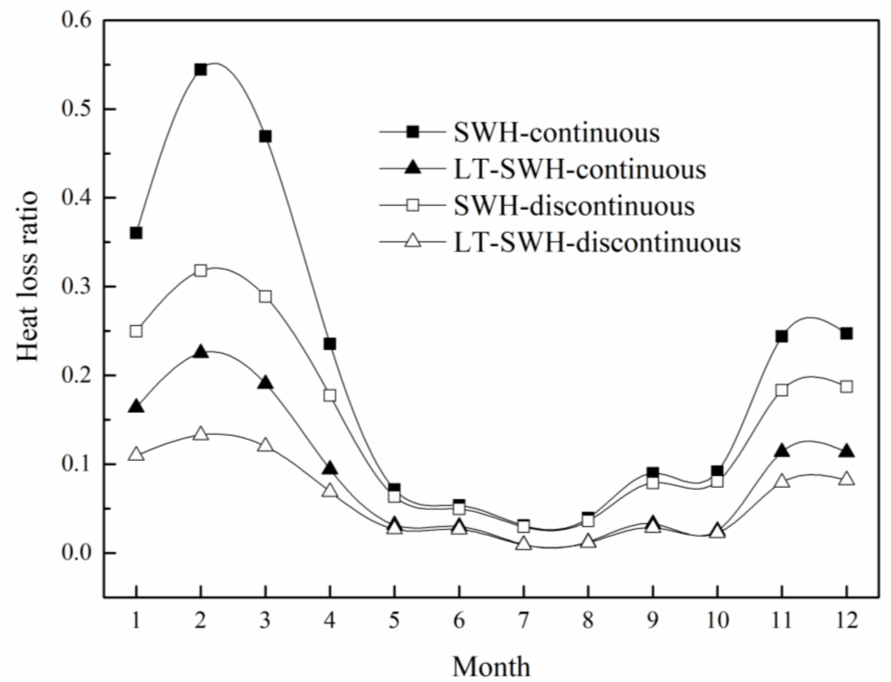

Fig.8. Comparison of heat loss ratios under different heating modes

The heat loss ratios, which are defined as the heat loss at night to the heat collection in the day, are presented in Fig.8. One can see that the trends of the curves are similar to that in Fig.7. However, because the nighttime heat loss directly determines the initial water temperature of the next day and further influences the daytime performance of the next day, the proportion is a little different. Besides, the ratios of the nighttime heat loss to the maximum heat collection (corresponding to heat collection under the discontinuous heating mode) are also presented for reference to some extent despite they are not accurate. By calculation, for the SWH system, the values of maximum and minimum heat loss ratio are 54.43% and 3.09%, respectively; while for the LT-SWH system, the values are 22.52% and 0.96%, respectively. It is further calculated that for the SWH system, the average annual heat loss ratio is 15.07%; while for the LT-SWH system, it is 6.15%. As a reference, the annual heat loss ratio, corresponding to the maximum heat collection, for the SWH system is 12.43%, while for the LT-SWH system is 5.00%.

From Fig.7 and Fig.8, one can further conclude that under the continuous heating mode, the nighttime heat loss of the SWH system is at least two times of the LT-SWH system; correspondingly, the difference of the effective heat gain is at least 13%. However, the results of Fig.6 show that from November to April, the effective heat gains of that two systems are approximately in the same month, the difference is within 4%. The big heat loss coefficients of LT-SWH system and SWH, which are functioning at different times, are responsible for that.

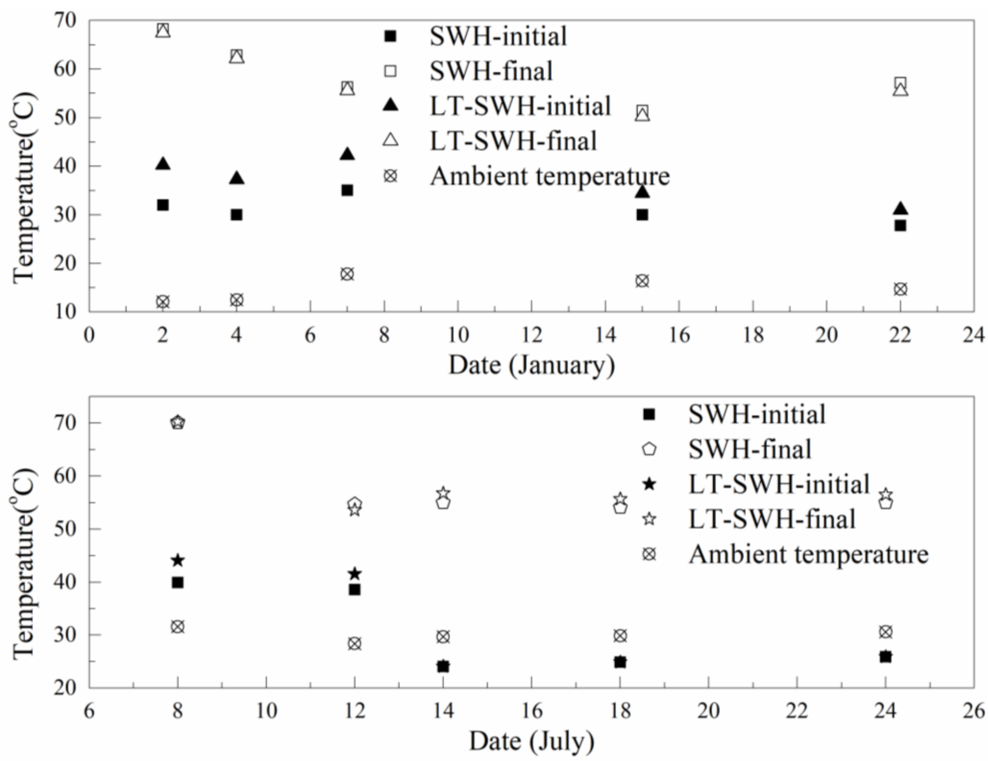

Fig.9. Comparison of the initial temperatures and final temperatures in January and July

To verify the inference, the initial and final water temperatures of selected days in January (above) and July (down) are respectively illustrated in Fig.9.

In January, the water temperatures of the effective five supplying days are chosen. From

Fig.9, one can see that the initial water temperatures of the LT-SWH system are obviously higher than that of the SWH system on the same day; however, the final water temperatures of that two systems are approximately equal. For the former, the heat loss of the solar collector of LT-SWH system, which is dominant in the total heat loss, is negligible due to the thermal diode property of loop thermosyphon. Therefore, after a night of dissipation, the initial water temperature of the LT-SWH system is higher. This pattern is sensitively responded by the first and the second points. However, the higher initial water temperature also acts on the daytime heat loss of the LT-SWH system, leading to a lower photothermal efficiency and therefore a smaller temperature rise. In other words, under the continuous heating mode, the heat energy reserved by the loop thermosyphon at night will be mostly dissipated in the day. Therefore, the final temperatures are approximately for the two systems. A similar cycling pattern also happens from November to April and it is why the two systems have the approximate values of the effective heat gain during those months.

The big heat loss coefficients of the two systems functioning at different times are also clearly illustrated in July. As shown in the bottom of Fig.9, the latter three days of the two system have the same initial water temperatures, but the final water temperatures of the LT-SWH system are higher than that of the SWH system because of the comparatively higher photothermal efficiency. However, for the former two points, they share the same cyclical pattern with January. The difference is, from May to October, the effective heat gains in these months of the LT-SWH system are bigger than that of the SWH system in the same month due to the bigger effective number of supplying days.

4.3 Comparison of photothermal efficiency

The average monthly photothermal efficiencies of the SWH system and the LT-SWH system under different heating modes are shown in Fig.10. It indicates that firstly, the monthly photothermal efficiency of the LT-SWH system is higher than that of the SWH system corresponding to the same month under the discontinuous heating mode. Secondly, the efficiencies of the two systems are all no less than their corresponding typical photothermal efficiencies, which seems counterintuitive to some extent. In general, compared with ambient temperature, the municipal water in China has the characteristic of warm in winter and cool in summer (Qiu, 2017), which resulting that the expected photothermal efficiency is usually higher than the typical photothermal efficiency in summer but smaller than the typical photothermal efficiency in winter. However, the water temperature of the local river, which is employed in the simulation in this study, is usually smaller than the municipal water temperature and the average ambient temperature most of times. It is responsible for the counterintuitive perception. Finally, under the continuous heating mode, the photothermal efficiencies of the LT-SWH system and the SWH system both show a trend of increase first and then decrease; meanwhile, similar to the trend of effective heat gain, the photothermal efficiencies of the LT-SWH system are approximately equal to the corresponding SWH system from November to April.

By calculation, under the continuous heating mode, the annual photothermal efficiency of the SWH system is 46.62%, while it is 48.37% for the LT-SWH system; under the discontinuous heating mode, the values are 56.52% and 59.53%, respectively.

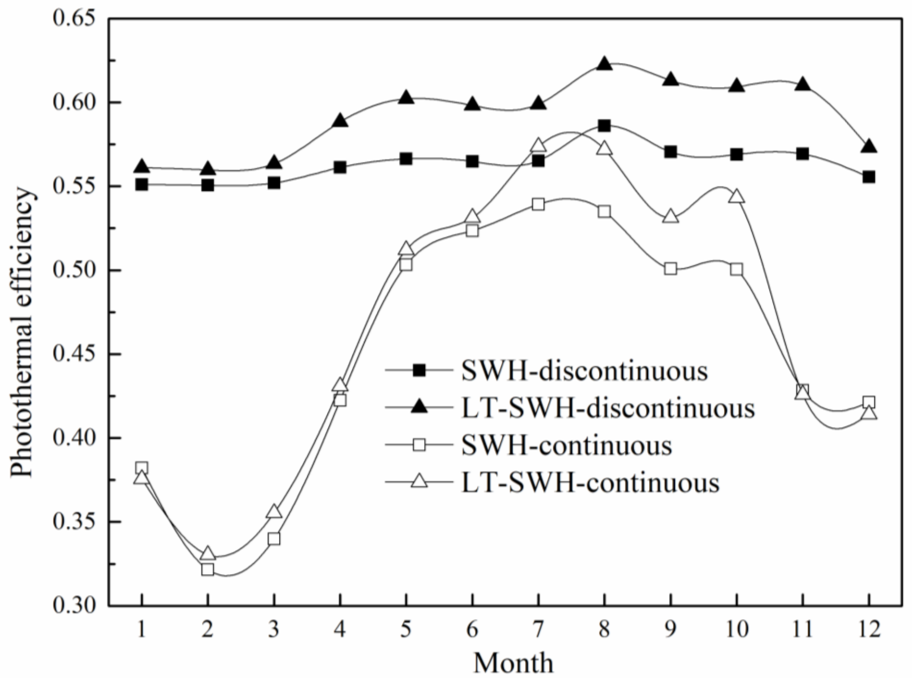

Fig.10. Comparison of monthly average thermal efficiencies under different heating modes

4.4 Influence of the set temperature

Under the continuous heating mode, the temperature setting will significantly affect the effective heat gain in the day and the heat loss at night. The variations of the effective number of supplying days with water temperature are displayed in Fig.11. It indicates that firstly, the effective number of supplying days decreases with increasing the set temperature. Correspondingly, for the LT-SWH system, the number of days decreases from 189 to 93 with the set temperature increasing from 45 °C to 65 °C; while for the SWH system, the number of days decreases from 187 to 95. The effective numbers of supplying days both decrease by around 50% for the two systems. Secondly, the difference of the effective number of supplying days between the LT-SWH system and the SWH system shows a trend of increases first and then decreases with increasing the set temperature; meanwhile, the difference is below zero when the set temperature is bigger than 65 °C. In brief, superiority of LT-SWH system varies with the set temperature, gradually diminishes when the set temperature is higher than 50 °C and reverses when set temperature is higher than a specific value between 60 °C-65 °C.

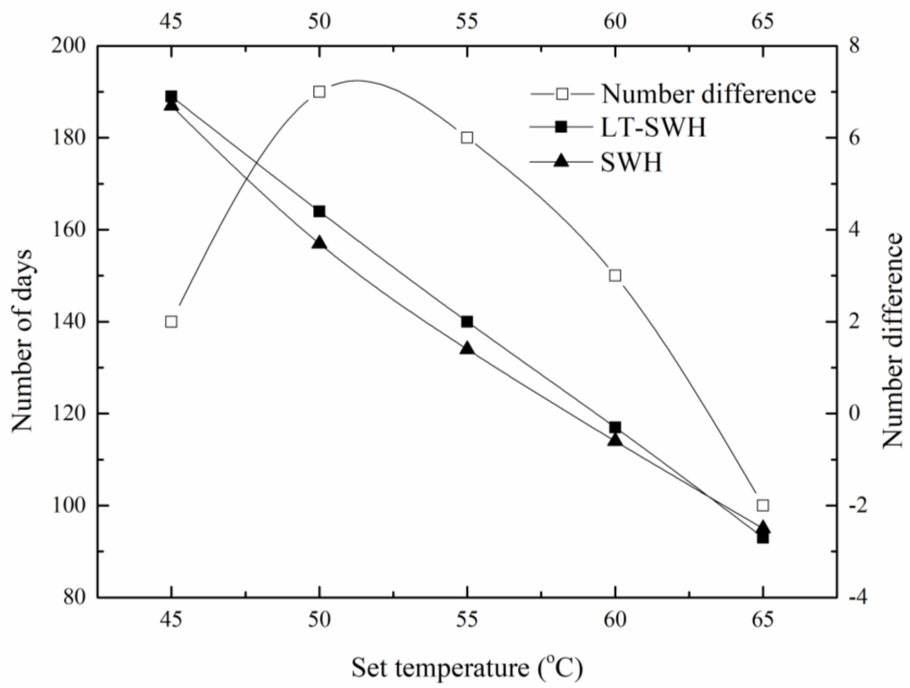

Fig.11. Variation of the effective number of supplying days with final water temperature

Variations of the annual cumulative effective heat gain and the annual cumulative heat loss with increasing the set temperature are presented in Fig.12. It is understandable that the annual cumulative effective heat gain decreases, while the annual cumulative heat loss correspondingly increases, with increasing the set temperature. When the set temperature rising from 45 °C to 65 °C, the annual cumulative effective heat gain decreases nearly 32% for the LT-SWH system, while nearly 26% for the SWH system; correspondingly, the annual cumulative heat losses respectively increase 158% and 165% for that two systems. The nighttime heat loss is more sensitive to the set temperature. One can further conclude that contrary to the cyclical patterns presented in Fig.6 and Fig.9, the big heat loss caused by the higher set temperature at night will be offset in the day to some extent.

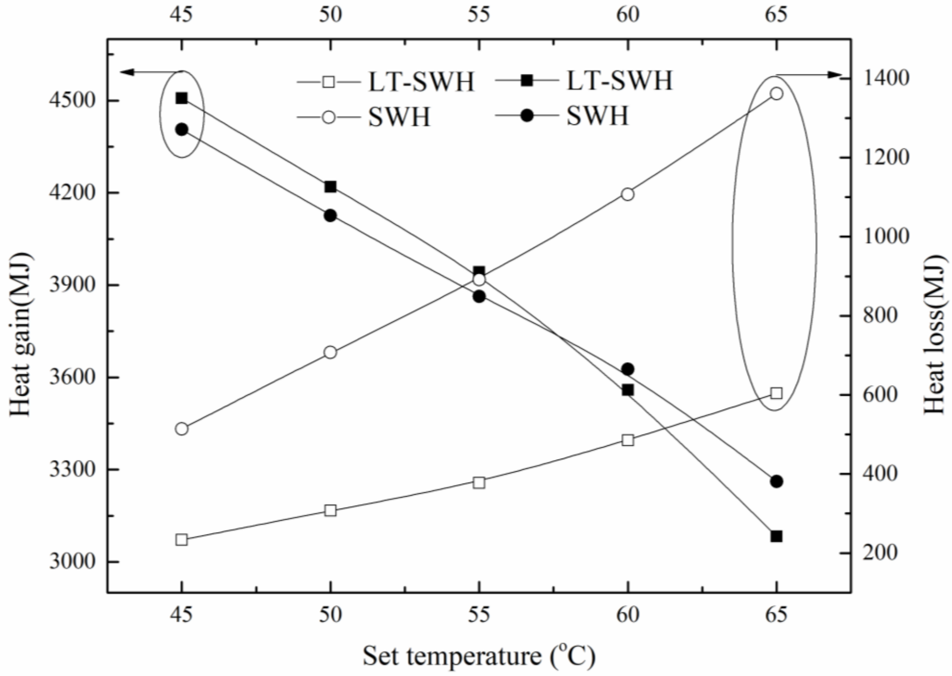

Fig.12. Variation of the annual cumulative heat gain and heat loss with increasing set temperature

Besides, Fig.12 exhibits that the difference of effective heat gain between the LT-SWH system and SWH system decreases with increasing the set temperature; while the difference of nighttime heat loss increases with increasing the set temperature. The interaction leads to a fact that the effective heat gain of the LT-SWH begins to become smaller than that of the SWH system when the final water temperature is no less than 60 ℃. One can note that compared to the effective number of supplying days, the effective heat gain reverses at a lower set temperature. In summary, the mismatch between the differences clearly shows that under the continuous heating mode, for the LT-SWH system, the decisive advantage of the lower heat loss at night gradually fades away and the bigger daytime heat loss gradually begins to dominate the dominance with increasing the set temperature.

The reasons for such variations in Fig.11 and Fig.12 can also refer to the variations in effective heat gain shown in Fig.6 and Fig.9. That is, compared with the SWH system, the heat energy reserved by the loop thermosyphon at night will be mostly or totally dissipated in the day; and even worse, the bigger daytime heat loss becomes negative to the system performance when the set temperature is big enough.

To verify that in detail, when increasing the set temperature, the average annual initial water temperature and average annual final water temperature of two systems, as well as the average annual temperature drops at night and the average annual temperature rises in the day, are respectively presented in Fig.13 and Fig.14.

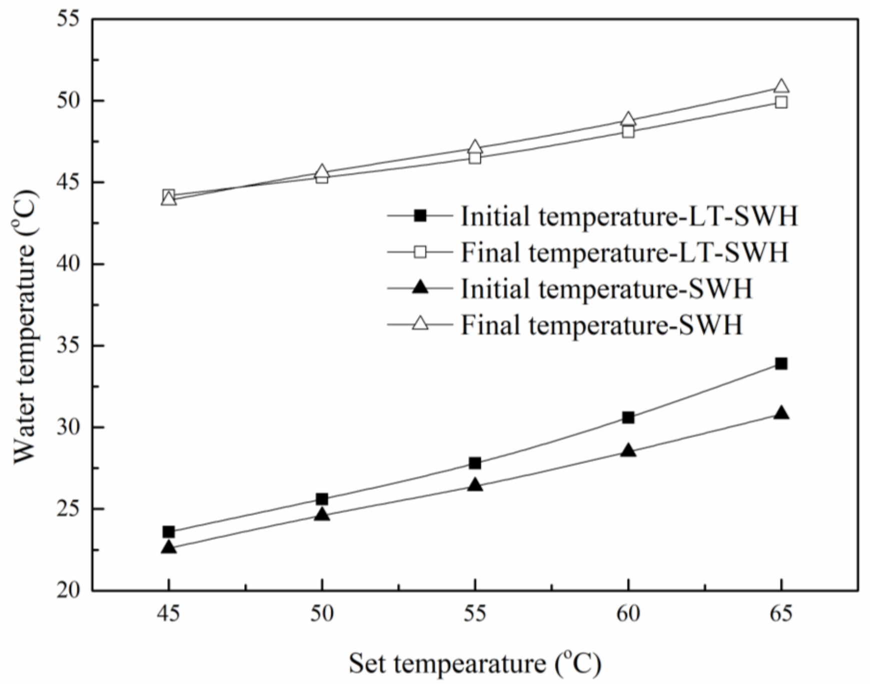

Fig.13. Variations of the average annual initial water temperature and final water temperature with increasing set temperature

From Fig.13, one can observe that variations in the average annual initial and final water temperatures share the similar trend with Fig.9. That is the LT-SWH system has higher initial water temperature because of the smaller nighttime heat loss, but lower final water temperature because of the bigger daytime heat loss. Meanwhile, the differences of the initial temperature and the final temperature between the two systems both increase as expected with increasing the set temperature.

From Fig.14, it is expected that for the two systems, increasing the set temperature increases the average annual temperature drop but decreases the average annual temperature rise. However, the increasing and decreasing gradients are different. As can be seen from Fig.14 that when the set temperature rising from 45 ℃ to 65 ℃, the average annual temperature drop of the LT-SWH system rises from 2.1 ℃ to 3.5 ℃, while the SWH system rises from 4.6 ℃ to 8.0 ℃. The gradient of temperature drop of the LT-SWH system is smaller. Correspondingly, the average annual temperature rise of the former decreases from 20.6 ℃ to 16.0 ℃, while it is from 21.3 ℃ to 19.9 ℃

for the latter. Obviously, the gradient of temperature rise of the LT-SWH system is bigger. Again, as mentioned before, the big heat loss coefficients functioning at different times acts as a mediator. It leads to a certainty that there must be an intermediate temperature, at which the effective heat gain of the two systems equals to each other. From Fig.14, one can conclude that the value is between 55-60 ℃. The performs of initial and final water temperature support the conclusion above.

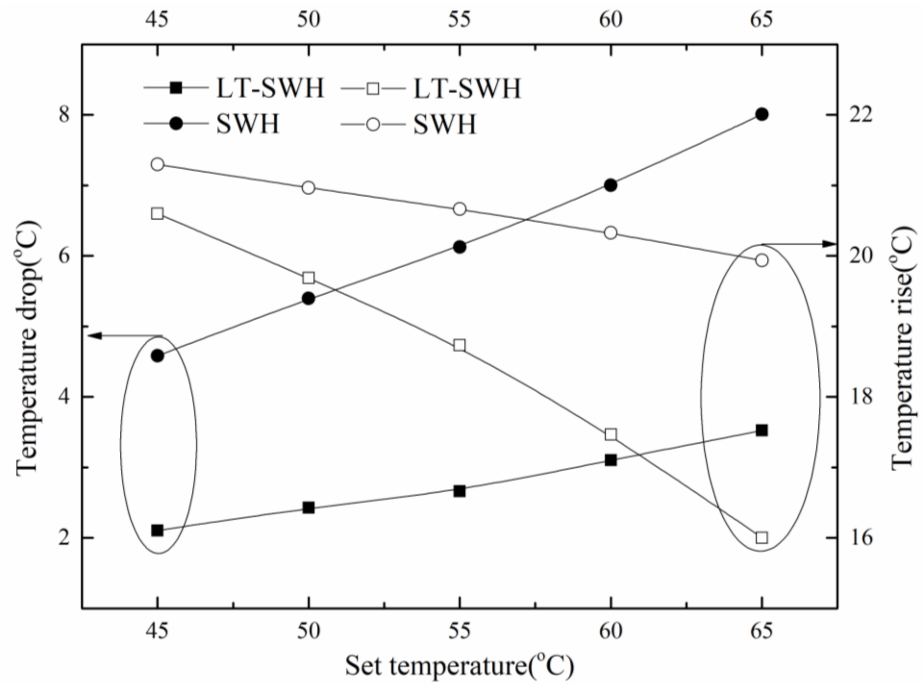

Fig.14. Variations of the average annual temperature rise and temperature drop with the increasing set temperature

4.5 Static payback period

Compared with the conventional electric water heater and the gas water heater, the static payback periods of the two systems are analyzed in the presented study. The prices of the electricity and the natural gas refer to the second level of the civil price, which are respectively announced by the Fujian province's power grid and the Fuzhou development and reform commission. The prices are 0.5483 RMB/(kWh) and 4.16 RMB/m^3, respectively. The calorific value of natural gas in China is 34 MJ/m^3. And the thermal efficiency of the gas water heater is 0.88 (Zhou and Qin, 2016), while the thermal efficiency of the electric water heater is 0.9 (Hu et al., 012). Effective heat gains when set temperature is 48 ℃ are referenced. The initial investments of the SWH system and the LT-SWH system are about RMB 2300 and RMB 2900, respectively. The cost of the SWH system consists of the collector (RMB 1000), solar water tank (RMB 800), pipelines and construction costs (RMB 500); while the LT-SWH system consists of the collector(RMB 1000), solar water tank with spiral coil (RMB 1200), refrigerant (RMB 100), pipelines and construction costs (RMB 600). Table 2 lists the results.

Table 2. The static payback periods of SWH system and LT-SWH system

Heating mode		Annual Heat Gain（MJ）	Electric Water Heater（year）	Gas Water Heater（year）
Discontinuous	SWH	5114.3	2.7	3.2
	LT-SWH	5387.4	3.2	3.9
Continuous	SWH	4218.5	3.2	3.9
	LT-SWH	4377.2	3.9	4.8

It can be seen from Table 2 that for the SWH system and the LT-SWH system, there are relatively short static payback periods when compared with the electric water heater. It is because the price of natural gas per MJ energy is nearly 80% more than that of the electric. Besides, compared with the SWH system, the LT-SWH system has a longer static payback period under the same heating mode, but the difference is within a year. On the whole, for the SWH system, static payback period ranges between 2.7-3.9 years; while for the LT-SWH system, it is 3.2-4.8 years. However, considering that the LT-SWH system is free of corrosion and freezing problems when Heating, the difference in the period between the two systems is acceptable. The LT-SWH provides a promising substitute for building energy savings.

5 Conclusions

Compared with the SWH system, the LT-SWH system has a bigger heat loss coefficient at the daytime but a smaller heat loss coefficient at the nighttime. Interaction of above is rarely reported based on long-term running. In this study, based on the typical meteorological year data of Fuzhou city, the annual performances of the SWH system and the LT-SWH system, under the continuous and discontinuous heating modes, are comparatively analyzed. Variations in the effective heat gain and the effective number of supplying days are discussed on the premise that the two systems have the approximate typical photothermal efficiencies. The main conclusions are below:

1) Under the discontinuous and continuous heating modes, the annual effective numbers of supplying days of the SWH system are 139 and 168, respectively; while they are 153 and 173, respectively, for the LT-SWH system.

2) Under the discontinuous heating mode, the effective heat gain of the SWH system is

always smaller than that of the LT-SWH corresponding to the same month. However, under the continuous heat mode, the monthly effective heat gains of the SWH system are approximate to that of the LT-SWH system from November to April. The big heat loss coefficients functioning at the different times is responsible for that. By calculation, the average annual heat loss ratio is 15.07% for the SWH system and 6.15% for the LT-SWH system.

3) The temperature setting not only significantly affects the effective heat gain but also changes the relative magnitudes of the two systems. The effective heat gain of the LT-SWH begins to smaller than that of the SWH system when the final water temperature is no less than 60 ℃.

4) The static payback period of the LT-SWH system, which ranges between 3.2-4.8 years, is a little longer than that of the SWH system.

In conclusion, despite the LT-SWH system operates free of corrosion and freezing problems, it is conditional to substitute with the conventional SWH system, especially when the water temperature on demand is high.

Acknowledgment

This work has been sponsored by the Shanghai Sailing Program (18YF1409100), Shanghai Local Capacity Building Program (18020501000), which are gratefully acknowledged by the author.

Declarations of interest: none

References:

Cook J., 1985. Passive cooling. MIT Press, London (UK).

Duffie J. A., Beckman W. A., 2006. Solar engineering of thermal processes (3rd ed). John Wiley &Sons, New Jersey.

Fan Jianhua, Furbo Simon, 2012a. Buoyancy driven flow in a hot water tank due to standby heat loss. Sol. Energy. 86, 3438–3449.

Fan Jianhua, Furbo Simon, 2012b. Thermal stratification in a hot water tank established by heat loss from the tank. Sol. Energy. 86, 3460–3469.

G.L. Morrison, 1986. Reverse circulation in thermosyphon solar water heaters. Sol. Energy. 36(4), 377-379.

He Wei, Zhang Yang, Ji Jie, 2011. Comparative experiment study on photovoltaic and thermal solar system under natural circulation of water. Appl. Therm. Eng. 31(16), 3369-3376.

GB/T 19141-2003.Technical conditions of domestic solar hot water system.

Hu Yunpin, Wan Jing, Tang Jincai, Wang Di, 2012. Economic evaluation of solar hot water project in wuhan area. Acta Energiae Solaris Sinica, 33(6), 916-921.

Huang B.J., Du S.C., 1991. A performance test method of solar thermosyphon systems. J. Sol. Energ. –T. ASME. 113(3), 172-179.

Ioannis Michaelides, Polyvios Eleftheriou, George A. Siamas, George Roditis, Paraskevas Kyriacou, 2011. Experimental investigation of the night heat losses of hot water storage tanks in thermosyphon solar water heaters. J. Renew. Sustain. Ener. 3, 033103.

Jinzhi Zhou, Xudong Zhao, YanpingYuan, Jing Li, MinYu, YiFan, 2020. Operational performance of a novel heat pump coupled with mini-channel PV/T and thermal panel in low solar radiation. Energ. Built. Environ. 1(1), 50-59.

Klein S. A., 1975. Calculation of Flat-Plate Loss Coefficients. Sol. Energy. 17(1), 79-79.

Kok Seng Ong, Kevin Osmond, Wei Li Tong, 2015. Revserse flow in natural convection heat pipe solar water heater. Int. J. Low-Carbon. Tec. 10(4), 430–437.

Li Kefeng, Hao Shenghong, Zhuang Chunyi, Pu Ling, 2006. A new formula for estimating water temperature in natural river channel by using meteorological factors. J. Sichuan Uni. (Eng. Sci. Ed.). 38(1),1-4.

Morrison G.L., 1986. Reverse circulation in thermosyphon solar water heater. Sol. Energy. 37(4), 377–379.

Nada S. A., El-Ghetany H. H., Hussein H M S, 2004. Performance of a two- phase closed thermosyphon solar collector with a shell and tube heat exchanger. Appl. Therm. Eng. 24(13), 1959—1968.

Qiu Guoquan, Xia Yanjun, Yang Hongyi, 2001. Optimization calculation of solar radiation model in sunny days, Acta Energiae Solaris Sinica. 22(4), 456-460.

Qiu Zhan, 2017. Development Status and Application Prospect of Sewage Source Heat Pump in Shanghai (In Chinese). Urban Roads Bridges and Flood Control. 4, 110-112.

Raisul Islam M., Sumathy K., Ullah Khan S., 2013. Solar water heating systems and their market trends. Renew Sust Energ Rev. 17, 1–25.

Rejane De Cesaro Oliveski, Arno Krenzinger, Horacio A Vielmo, 2003. Cooling of cylindrical vertical tanks submitted to natural internal convection. Int. J. Heat Mass Tran. 46, 2015–2026.

Sadhishkumar S., Balusamy T, 2014. Performance improvement in solar water heating systems—a review. Sust.

Energ. Rev. 37, 191–198

Tang Runsheng, Yuan Yuqin, 2014. Nocturnal reverse flow in water-in-glass evacuated tube solar water heaters. Energ. Convers. Manage. 80, 173–177.

Tang Runsheng, Cheng Yanbin, Wu Maogang, Li Zhimin, Yu Yamei, 2010. Experimental and modeling studies on thermosyphon domestic solar water heater with flat-plate collectors at clear nights. Energ. Convers. Manage. 51, 2548–2556.

Vaxman M., Sokolov M., 1986. Effects of connecting pipes in thermosiphonic solar systems. Sol. Energy. 37(5), 323–330.

Wang Ling, Wang Zhaoguo, 2008. Discussion on calculation parameters of solar water heater total area in Shanghai area (in Chinese). Water Wastewater Eng. 34(12), 124-126.

XiaojiaoYang, Liangliang Sun, YanpingYuan, Xudong Zhao, Xiaoling Cao, 2018. Experimental investigation on performance comparison of PV/T-PCM system and PV/T system. Renew. Energ. 119, 152-159.

Zhang Hefei, 2004. Solar thermal utilization principle and computer simulation(Second Edition), Northwestern Polytech. Univ. Press, Xi 'an. 93-98.

Zhang Tao, Pei Gang, Zhu Qunzhi, Ji Jie, 2016. Investigation on the optimum volume-filling ratio of a loop thermosyphon solar water-heating system. J. Sol. Energ. –T. ASME. 138(4), 041006.

Zhang T., Zhu Q. Z., Pei G., Ji J., 2017a. Annual performance comparison between solar water heating system and solar photovoltaic/thermal system- A case study in Shanghai city. Int. J. Low-Carbon. Tec. 12(4), 420-429.

Zhang Tao, Zhu Qunzhi, Zhang Suyang, Pei Gang, Ji Jie, 2017b. Comparative experimental study of loop thermosyphon PV/T system and common PV/T system. Acta Energiae Solaris Sinica. 38(12), 3251-3258.

Zhou Yu, Qin Chaokui, 2016. Comparison of performance test of gas-fired hot water heater under pure methane and natural gas conditions in Shanghai area (In Chinese). Gas Tech.. 498, 4-7.